Basin-scale distribution of prokaryotic phylotypes in the epipelagic layer of the Central South Pacific Ocean during austral summer

Yuya Tada*[1], Takuhei Shiozaki[2, 3], Hiroshi Ogawa[2], and Koji Suzuki[1]

[1]Faculty of Environmental Earth Science, Hokkaido University, North 10 West 5, Kita-ku, Sapporo, Hokkaido 060-0810, Japan

[2]Atmosphere and Ocean Research Institute, The University of Tokyo, 5-1-5 Kashiwanoha, Kashiwa-shi, Chiba 277-8564, Japan

[3]Research and Development Center for Global Change, Japan Agency for Marine-Earth Science and Technology, 2-15, Natsushima-cho, Yokosuka, Kanagawa 233-0061, Japan

*Corresponding author: Yuya Tada

E-mail: yuyatada@ees.hokudai.ac.jp

Phone: +81-11-706-2246

Fax: +81-11-706-3026

Abstract

In the present study, we used catalyzed reporter deposition-fluorescence *in situ* hybridization to quantify the abundance of five bacterial (*Alphaproteobacteria*, SAR11, *Gammaproteobacteria*, SAR86, and *Bacteroidetes*) and two archaeal (*Crenarchaeota*

23 and *Euryarchaeota*) phylotypes in the epipelagic layer (0–200 m) of the Central South
24 Pacific Ocean along 170°W from 0° to 40°S. We found that the distribution patterns of
25 these phylotypes differed from each other. All phylotypes except *Gammaproteobacteria*
26 were particularly abundant at the surface water of the equatorial region, whereas
27 *Gammaproteobacteria* was relatively abundant in the area from the southern part of the
28 South Pacific Ocean. SAR11, affiliated with *Alphaproteobacteria* was the dominant
29 phylotype at all depths, throughout the study area. The abundance of SAR11
30 significantly increased with chlorophyll *a* concentration, suggesting that phytoplankton
31 could affect their distribution pattern. There was a positive correlation between
32 *Bacteroidetes* abundance and water temperature, suggesting that the temperature
33 gradient could be a critical factor determining their distribution in the South Pacific
34 Ocean. *Crenarchaeota* and *Euryarchaeota* were more abundant at the equatorial region
35 than other study areas. *Euryarchaeota* abundance significantly decreased with depth,
36 and increased with chlorophyll *a* concentration. It suggests that there was ecological
37 interaction between *Euryarchaeota* and phytoplankton in the equatorial surface. Our
38 data indicate that distinct hydrographic properties such as seawater temperature, salinity,
39 and the concentrations of chlorophyll *a* and nutrients can principally control the
40 basin-scale distribution of different prokaryotic phylotypes in the epipelagic layer of the
41 Central South Pacific Ocean.
42
43
44

Keywords: Marine bacteria; Marine archaea; Fluorescence *in situ* hybridization; Central South Pacific Ocean

Heading: Bacterial and archaeal distribution in the Central South Pacific Ocean

1. Introduction

Bacteria and Archaea are widely recognized as important players of oceanic biogeochemical processes that are involved in the organic matter and nutrient cycling in the ocean. Previous studies reported that prokaryotic biomass and production vary with certain basin-scale hydrographic gradients in the ocean (e.g., Teira et al. 2006a; Schattenhofer et al. 2009; Yokokawa et al. 2013). In the Atlantic Ocean, vertical and horizontal distribution patterns of specific prokaryotic lineages have been characterized in several basin-scale studies (Teira et al. 2006a; Schattenhofer et al. 2009; Morris et al. 2012). In these studies, SAR11 and *Prochlorococcus* were reported as dominant within prokaryotic assemblages at the surface, while SAR202 and *Crenarchaeota* were predominant in the meso- and bathypelagic layers, deeper than 200 m. With regard to horizontal distribution, the relative abundance of *Gammaproteobacteria* and *Bacteroidetes* increased in the Northern Atlantic Drift province (Schattenhofer et al., 2009). This suggests that distinct hydrographic features of oceanic provinces (e.g. the South Atlantic Gyral, Western Tropical Atlantic, and North Atlantic Gyral provinces) could be important contributors to the distribution pattern of prokaryotic phylotypes in the Atlantic Ocean. However, the basin-scale distribution of bacterial and archaeal phylotypes has not yet been investigated in the epipelagic layer of the Central South Pacific Ocean.

The South Pacific Ocean is divided into five distinct provinces, called the Pacific Equatorial Divergence, the South Pacific Subtropical Gyre, the South Subtropical Convergence, the Subantarctic, and the Antarctic, based on prevailing

71 physical forces (Longhurst 2010). Primary productivity is generally high in the Pacific
72 Equatorial Divergence due to the equatorial upwelling, while the South Pacific
73 Subtropical Gyre contains a huge nutrient-limited ecosystem in the Pacific Ocean
74 (Moore et al. 2001). As in the Atlantic Ocean, the Southern Pacific also has a steep
75 latitudinal gradient of hydrographic features such as temperature, salinity, and
76 concentrations of nutrients and chlorophyll *a* (Chl *a*), suggesting that these
77 biogeographical features could affect the basin-scale distribution of bacterial and
78 archaeal phylotypes.
79 During the last decade, genomic and isotopic studies have demonstrated that
80 marine bacterial and archaeal phylotypes possess distinct metabolic systems to acquire
81 energy from various sources. For instance, phylotypes of SAR11 (affiliated with
82 *Alphaproteobacteria*), SAR86 (affiliated with *Gammaproteobacteria*), and
83 *Flavobacterium* (affiliated with *Bacteroidetes*) are capable of harvesting energy from
84 light using proteorhodopsin (Gòmez-Consarnau et al. 2007; Campbell et al. 2008;
85 González et al. 2008; Dupont et al. 2012; Yoshizawa et al. 2012). In addition,
86 *Bacteroidetes* lineages possess several enzymes that degrade polymeric substrates
87 (Bauer et al. 2006), and can proliferate in response to phytoplankton blooms in coastal
88 waters (Pinhassi et al. 2004; Grossart et al. 2005; Tada et al. 2011). On the other hand,
89 genomic studies on a marine non-extremophilic archaeon, *Nitrosopumilus maritimus*,
90 suggest that the *Crenarchaeota* phylotype should be a chemoautotroph that can acquire
91 energy through ammonia oxidation (Könneke et al. 2005; Walker et al. 2010). A
92 previous metagenomics study also indicated that genes encoding rhodopsin are present

93 in marine *Euryarchaeota* (Iverson et al. 2012). In addition, isotopic studies showed that
94 both archaeal lineages metabolized organic substrates such as amino acids in natural
95 environments (Herndl et al. 2005; Teira et al. 2006b; Varela et al. 2008). These studies
96 indicate that different prokaryotic phylotypes are possibly involved in distinct cycles of
97 organic and inorganic matter in the ocean. Therefore, an investigation of the latitudinal
98 and depth distribution of specific bacterial and archaeal phylotypes would facilitate a
99 better understanding of the linkage between microorganisms and biogeochemical
100 processes in the Central South Pacific Ocean.
101 The objective of this study was to quantify the abundance of five bacterial
102 (*Alphaproteobacteria*, SAR11, *Gammaproteobacteria*, SAR86, and *Bacteroidetes*) and
103 two archaeal (*Crenarchaeota* and *Euryarchaeota*) phylotypes along a transect, from the
104 equator to the southern extremity of the Pacific Ocean. We collected samples from the
105 study area in the austral summer of 2013 and performed catalyzed reporter deposition
106 (CARD)-fluorescence *in situ* hybridization (FISH) (Pernthaler et al. 2002; Teira et al.
107 2004), which allows the identification and quantification of phylotype-specific
108 prokaryotic cells using fluorescence-labeled oligonucleotide probes.
109
110 **2. Materials and methods**
111 **2.1. Study sites and sample collection**
112 Seawater samples were collected using 10-l Niskin bottles (General Oceanics, FL) at
113 eight stations along a transect in the Central South Pacific Ocean along 170°W, from 0°
114 to 40°S during the KH-13-7 (December 11, 2013–February12, 2014) expedition of the

115 R/V *Hakuho-maru* (Fig. 1 and Table 1). Bacterial samples were collected from 0 or 5,
116 10, 20, 50, 100, and 200 m below the surface as well as the subsurface chlorophyll
117 maximum (SCM) layers. Archaeal samples were collected from the same sampling
118 layers for eubacteria, except for 0 or 5, and 20 m. Seawater samples were fixed with 2%
119 (v/v) paraformaldehyde, and stored at 4°C for 2 h. Fixed seawater samples (10–30 ml)
120 were then filtered through 0.2-µm pore size polycarbonate membrane filters (25 mm,
121 type GTTP, Millipore, Cork, Ireland), and stored at –80°C until further analysis.
122
123 **2.2. Environmental factors and total prokaryotic abundance**
124 Environmental factors except for primary productivity were measured at 0,
125 5, 10, 20, 30, 40, 50, 75, 100, 125, 150, and 200 m depths and the SCM layer. Water
126 temperature, salinity, and dissolved oxygen concentration were measured with a CTD
127 system (SBE, Sea-Bird Electronics). Seawater samples were filtered at < 14 kPa
128 through Whatman GF/F filters and Chl *a* was extracted from the filters with
129 *N*,*N*-dimethylformamide at 4°C for 24 h in the dark (Suzuki and Ishimaru 1990). Chl *a*
130 concentration was determined fluorometrically (Welschmeyer 1994). Samples for
131 macronutrient analysis were collected in 10-ml acrylic tubes and stored at –20°C until
132 further analysis on land, to estimate concentration of nitrate plus nitrite (NO_3 + NO_2),
133 nitrite (NO_2), ammonium (NH_4), and phosphate (PO_4) using a segmented
134 continuous-flow analyzer (QuAAtro, SEAL Analytical, Ltd.; Ogawa et al. 1999). The
135 nitrate (NO_3) concentrations were obtained by subtracting NO_2 values from NO_3+NO_2
136 data. Primary productivity was estimated by ^{13}C-labeling method (Hama et al. 1983) at

100%, 25%, 10%, 1%, and 0.1% photosynthetically active radiation (PAR) levels relative to the surface. Briefly, duplicate seawater samples were collected in acid-washed, 4.5-l polycarbonate bottles and ^{13}C-labeled sodium bicarbonate (99 atom % ^{13}C; Cambridge Isotope Laboratories, Andover, MA) was added to each bottle at a final concentration of 10 nmol·l^{-1}. Bottles were then incubated for 24 h with adjusting light levels in an on-deck incubator cooled by flowing surface seawater. The analytical procedures were followed as previously described (Shiozaki et al. 2009). To quantify total prokaryotic abundance, filters (10 ml seawater filtration) were stained with 4',6-diamidino-2-phenylindole (DAPI) mix consisting of 5.5 parts (vol/vol) Citifluor (Citifluor Ltd., London, United Kingdom), 1 part Vectashield (Vector Labs, Burlingame, CA), and 0.5 parts phosphate-buffered saline (PBS) supplemented with 2 μg·ml^{-1} DAPI. Finally, images of the filters were captured using a BZ9000 epifluorescence microscope equipped with a CCD camera (Keyence, Tokyo, Japan).

2.3. CARD-FISH

The abundance of each phylotype was determined by CARD-FISH (Pernthaler et al. 2002; Teira et al. 2004). Briefly, filters (30 ml seawater filtration) were first embedded in 0.1% (w/v) low-melting point agarose (Nacalai Tesque, Kyoto, Japan), dehydrated for 1 min with 95% ethanol, and dried completely. To quench endogenous peroxidase, filters were treated with 0.01% HCl for 10 min at room temperature and then washed with 50 ml Milli-Q water for 15 min. Filters were then treated with 10 mg·ml^{-1} lysozyme in Tris-ethylenediaminetetraacetic acid (EDTA) (TE) buffer (consisting of

159 10 mmol·l^{-1} Tris-HCl and 1 mmol·l^{-1} EDTA, pH 8.0) at 37°C for 60 min for bacterial
160 samples, or with 10.9 mg·ml^{-1} proteinase K in TE buffer at 37°C for 60 min for
161 archaeal samples. The filters were then washed for 60 min with 50 ml Milli-Q water
162 (three times for archaeal samples), dehydrated with 95% ethanol, cut into small pieces,
163 and hybridized with oligonucleotide probes labeled with horseradish peroxidase. Probes
164 were prepared at 0.28 ng·µl^{-1} in 300 µl hybridization buffer, containing 900 mmol·l^{-1}
165 NaCl, 20 mmol·l^{-1} Tris-HCl at pH 7.5, 10% (wt/vol) dextran sulfate, 0.02% (wt/vol)
166 sodium dodecyl sulfate (SDS), 1% (vol/vol) blocking solution (blocking reagent in 100
167 mM maleic acid, 150 mM NaCl), and formamide (FA). The FA concentration
168 appropriate for each probe was determined from probeBase
169 (http://www.microbial-ecology.net/probebase/).
170 FISH probes were used that targeted bacteria affiliated with *Eubacteria*
171 (Eub338; 35% FA) (Amann et al. 1990), *Alphaproteobacteria* (Alf968; 20% FA) (Neef
172 1997), SAR11 (SAR11-441 probe; 15% FA) (Rappé et al. 2002), *Gammaproteobacteria*
173 (Gam42a; 35% FA) (Manz et al. 1992), SAR86 (SAR86-1249; 50% FA) (Eilers et al.
174 2000), *Bacteroidetes* (Cf319a; 35% FA) (Manz et al. 1996), *Crenarchaeota* (GI-554;
175 0% FA) (Massana et al. 1997) and *Euryarchaeota* (Eury806; 0% FA) (Teira et al. 2004)
176 along with a negative control (Non338; FA, 35%) (Wallner et al. 1993). The Alf968
177 probe targeting *Alphaproteobacteria* detects only a few members of the SAR11 clade in
178 the open ocean (SILVA TestPrime analysis; http://www.arb-silva.de/search/testprime/).
179 Hybridization was performed at 46°C for 12–15 h.
180 After hybridization, filters were washed at 48°C for 15 min in 50 ml

pre-warmed buffer consisting of 20 mmol·l^{-1} Tris-HCl pH 7.4, 5 mmol·l^{-1} EDTA, 0.01% SDS, and NaCl at a concentration of 80 mmol·l^{-1} (for Eub338, Non338, Gam42a, and Cf319a), 225 mmol·l^{-1} (for Alf968), 318 mmol·l^{-1} (for SAR11-441), 28 mmol·l^{-1} (for SAR86-1249), or 900 mmol·l^{-1} (for GI-554 and Eury806). EDTA was omitted for reactions with SAR11-441 and two archaeal probes. Subsequently, filters were washed with 50 ml of 0.05% (vol/vol) Triton X-100 in PBS (PBST) and then incubated at 46°C for 45 min in PBS containing 10% (wt/vol) dextran sulfate, 2 mol·l^{-1} NaCl, 0.1% (vol/vol) blocking solution (blocking reagent in 100 mM maleic acid, 150 mM NaCl), 0.0015% (vol/vol) H_2O_2, and 0.7% (vol/vol) Alexa 488-labeled tyramide (amplification buffer). Filters were then washed for 15 min in 50 ml PBST, rinsed with Milli-Q water, air-dried, stained with DAPI mix, and photographed using epifluorescence microscope as described above.

2.4. Image analysis for cell counts

Epifluorescence microscopic images were stored as TIFF files and analyzed using the image analysis software Image J (version 1.48, National Institutes of Health, Bethesda, Maryland, USA) to obtain cell counts. Exposure times were optimized using samples with the negative control (Non338) probe. Image processing included three spatial filters: Laplacian (Kernel 5 × 5), Gaussian (Kernel 3 × 3), and median (radius 1) filters (Fazi et al. 2008). The newly created binary images for DAPI and FISH were edited in the overlay mode and overlapped cells were counted as FISH-positive cells. At least 10 images were analyzed for each sample.

2.5. Phylotype abundance and water-column integrated cell number

The each phylotype abundance was calculated using their proportion (i.e., percentage of each phylotype to DAPI-stained cells determined with the CARD-FISH analysis) and total prokaryotic abundance. Water-column integrated cell number of each phylotype was calculated by using the phylotype abundance of each sampling depth (7 and 5 depths for Bacteria and Archaea, respectively).

2.6. Statistical analysis

Data were analyzed in R software, version 3.1.0 (R Development Core Team 2011), using Spearman's rank correlation and multiple regression analyses to investigate the relationship between phylotype abundance and environmental factors. For multiple regression analysis, all data including the environmental parameters and the phylotype abundance were log (x+1)-transformed to approximate normal distribution. We used the Akaike information criterion (AIC: Akaike, 1974) for model selection, since the model minimizes the value of AIC and equivalently maximizes that of the log-likelihood minus the number of samples as a penalty. AIC model selection was performed using the MASS package (Venables and Ripley, 2002) in R software. The environmental factors used for statistical analysis were assumed to be independent of each other.

3. Results

3.1. Environmental characteristics and total prokaryotic abundance

Distribution of water temperature, salinity, dissolved oxygen, Chl *a*, primary productivity, concentrations of NO_3, NO_2, NH_4, PO_4, and prokaryote populations is shown in Fig. 2. Surface seawater temperature decreased from 30.3°C at Station 1 to 19.8°C at Station 9. Water temperature also generally decreased with depth, although the gradient was steeper at the equator than that in the south. An increase in salinity was observed with depth at Stations 3–4, reaching to > 36 at 100–200 m depth. Salinity decreased at Stations 8 and 9. Dissolved oxygen increased with latitude from north to south, and ranged from 3.9 $ml \cdot l^{-1}$ at 5 m depth at Station 1 to 4.9 $ml \cdot l^{-1}$ on the surface at Station 9. At Station 1, dissolved oxygen decreased sharply at depths of 100–200 m, presumably as a result of equatorial upwelling. The SCM layer declined from 41 m at Station 1 to 145 m at Station 5, but rose back to 82 m at Station 9. The highest Chl *a* concentration of 0.36 $\mu g \cdot l^{-1}$ was observed in the SCM layer at Station 1, possibly caused by the equatorial upwelling. In addition, primary productivity was highest (10.8 $\mu g\ C \cdot l^{-1} \cdot d^{-1}$) at the surface of Station 1. Surface primary productivity reduced southward from Station 1 to 4, but increased again at Stations 5–7 (from 3.7 to 6.1 10 $\mu g\ C \cdot l^{-1} \cdot d^{-1}$). The highest concentrations of NO_3 and PO_4 (14.5 µM and 1.09 µM, respectively) were observed at 200 m depth at Station 1. NO_2 concentration was relatively high in the surface layer (0–50 m), ranging from 0.28 to 0.32 µM. On the other hand, NH_4 concentration was relatively high at depths of 100–200 m at Station 4, ranging from 0.29 to 0.35 µM.

Total prokaryotic abundance ranged from 1.0×10^5 to 7.9×10^5 $cells \cdot ml^{-1}$. Prokaryotes were the most abundant at 100 m depth at Station 7. As for latitudinal

247 distribution, abundance was higher at Stations 1 and 7 than at other stations.

248

249 **3.2. Bacterial and Archaeal distributions**

250 *Eubacteria* accounted for 27%–89% of DAPI-stained cells (Fig. 3A). Water-column
251 integrated cell numbers of *Eubacteria* ranged from 4.42×10^{13} to 6.96×10^{13} cells·m^{-2},
252 the largest cell number was observed at Station 8 (Table 2). Eubacterial abundance
253 significantly increased with water temperature, and decreased with depth and
254 concentration of NO_3 and PO_4 (Table 3). As for latitudinal distribution, *Eubacteria*
255 count decreased at Station 7 and accounted for 57%–65% of DAPI-stained cells (5–50
256 m depths).

257 Relative abundance of *Alphaproteobacteria* decreased with depth and was
258 therefore, the most abundant at the surface, ranging from 0%–43% of DAPI-stained
259 cells throughout the area investigated (Fig. 3B). Their water-column integrated
260 abundance increased at Stations 1, 8, and 9 (1.70×10^{13} cells·m^{-2}, 1.93×10^{13} cells·m^{-2},
261 and 1.90×10^{13} cells·m^{-2}, respectively) (Table 2). The abundance significantly increased
262 with dissolved oxygen concentration, and decreased with salinity and concentrations of
263 NO_3 and PO_4 ($P < 0.05$, n = 56) (Table 3).

264 SAR11 clade was the most dominant bacterial lineage in the Central South
265 Pacific Ocean and accounted for 10%–55% of DAPI-stained cells at all depths
266 throughout the area investigated (Fig. 3C). This clade was particularly abundant at the
267 surface, accounted for an average of 38% ± 11% DAPI-stained cells. In addition, the
268 abundance exceeded 50% between 0 and 100 m depths at Stations 1, 5, 6, and 9. The

269 water-column integrated cell number of SAR11 as well as that of *Alphaproteobacteria*
270 increased at Station 8, and reached up to 3.90×10^{13} cells·m^{-2} (Table 2). The SAR11
271 abundance significantly increased with Chl *a* concentration ($P < 0.05$, n = 56) (Table 3).
272 In contrast, significantly negative correlations between their abundance and depth or
273 nutrient levels (NO_3, NO_2, or PO_4 concentration) were noted.
274 *Gammaproteobacteria* was particularly abundant in surface waters up to
275 100 m depth and accounted for 0.6%–7.9% of DAPI-stained cells (Fig. 3D). The
276 abundance at the surface layer increased southward from Station 4 and reached up to
277 7.9% at Station 8. In addition, their water-column integrated cell number increased at
278 southern part of the South Pacific Ocean (0.36×10^{13} cells·m^{-2} and 0.31×10^{13} cells·m^{-2}
279 at Stations 8 and 9, respectively) (Table 2). Gammaproteobacterial abundance was
280 negatively correlated with depth, salinity, and concentration of Chl *a* and nutrients
281 (except for NH_4) ($P < 0.01$, n = 56) (Table 3). In contrast, the abundance significantly
282 increased with dissolved oxygen ($P < 0.01$).
283 SAR86 clade was also relatively abundant in surface waters at Stations 1, 8,
284 and 9 (Fig. 3E). However, the abundance accounted for < 1% of DAPI-stained cells
285 between 0 and 100 m depths at Stations 3–7. Remarkably, relative abundance of this
286 clade increased at the SCM layer at Station 5 (2.0% of DAPI-stained cells). The
287 water-column integrated cell number of SAR86 ranged from 0.02×10^{13} cells·m^{-2} to
288 0.12×10^{13} cells·m^{-2}, and increased at Stations 1, 8, and 9 (Table 2). SAR86 abundance
289 significantly increased with dissolved oxygen ($P < 0.01$, n = 56), and decreased with
290 depth, salinity and NH_4 concentration ($P < 0.01$, $P < 0.01$, and $P < 0.05$, respectively)

(Table 3).

Relative abundance of *Bacteroidetes* was clearly higher near the surface than in waters more than 100 m depth and ranged from 0.2%–17% of DAPI-stained cells (Fig. 3F). The proportion decreased southward from Station 1, increased at Station 8 and reached 17% of DAPI-stained cells at 20 m depth. The largest water-column integrated cell number was observed at Station 1 (0.70×10^{13} cells·m^{-2}) (Table 2). Abundance of this phylotype was positively correlated with water temperature ($P < 0.05$, n = 56), and negatively correlated with depth, salinity, and concentrations of NO_3 and PO_4 ($P < 0.01$, $P < 0.05$, $P < 0.01$, and $P < 0.01$, respectively) (Table 3).

Crenarchaeota was more abundant at Station 1 than any other station (ANOVA, $P < 0.01$; Tukey's post-hoc, $P < 0.01$), and accounted for 2.6%–5.7% of DAPI-stained cells (Fig. 4A). Their water-column integrated cell number increased at Stations 1 and 9 (each 0.19×10^{13} cells·m^{-2}) (Table 2). However, the relative abundance of this phylotype was relatively stable at all stations except at Station 1.

Euryarchaeota accounted for 0.1%–3.9% of DAPI-stained cells (Fig. 4B) and was most abundant at 10 m depth, at Station 1. Also, their water-column integrated cell number increased at Station 1, and reached at 0.27×10^{13} cells·m^{-2} (Table 2). Their abundance significantly decreased with depth ($P < 0.01$, n = 40), and increased with Chl *a* concentration ($P < 0.01$) (Table 3).

3.3. Interrelationship between distribution of phylotypes and environmental factors

313 Results of multiple regression analysis indicate that hydrographic features (water
314 temperature, salinity, dissolved oxygen, Chl *a*, NO_2, HN_4, or PO_4) have a significant
315 effect on the distribution patterns of bacterial and archaeal phylotypes (Table 4). Since
316 there were strongly significant correlations between water temperature and depth (R = –
317 0.57, $P < 0.001$, n = 56, in Pearson's correlation analysis), and NO_3 and PO_4 (R = 0.96,
318 $P < 0.001$, n = 56), the factors selected for the regression model using the AIC included
319 water temperature, salinity, dissolved oxygen, Chl *a*, NO_2, NH_4, and PO_4. These
320 environmental factors explained 38%–63% of the distribution patterns of each
321 phylotype in this study ($P < 0.001$).
322
323 **4. Discussion**
324 **4.1. Distribution of bacterial lineages**
325 Our investigation of prokaryotes in the epipelagic layer revealed that the abundance of
326 bacterial and archaeal phylotypes in the South Pacific Ocean was significantly
327 correlated with several environmental factors (i.e., water temperature, salinity, dissolved
328 oxygen, Chl *a* and nutrients). This suggests that the hydrographic features are the
329 critical factors shaping the bacterial and archaeal distribution patterns.
330 We characterized Bacteria and Archaea using CARD-FISH, and detected
331 29%–91% of DAPI-stained cells using the probes Eub338, GI-554, and Eury806. A
332 possible reason for the relative inefficiency of detection is that many dead or decaying
333 cells might still remain the genomic DNA after rRNA degradation (del Giorgio and
334 Gasol 2008). Another possible reason is the limited range of Eub338 probe, which is

335 unable to detect *Planctomycetes* and *Verrucomicrobia*. These phylotypes can be
336 detected using Eub338II and Eub338III, respectively (Amann and Fuchs 2008). Thus,
337 the CARD-FISH method used in this study may have underestimated eubacterial
338 abundance.
339 Our results showed that SAR11 clade was the dominant group of
340 prokaryotes in the epipelagic layer (Fig. 3C). In addition, the abundance of this
341 phylotype was significantly correlated with Chl *a* concentration (Tables 3 and 4). This
342 implies that phytoplankton biomass could be a critical determinant of SAR11
343 abundance in our survey area. Additionally, these results are in agreement with data
344 obtained from the Atlantic Ocean (Eiler et al. 2009; Schattenhofer et al. 2009). Indeed,
345 genomic and metabolic analyses suggest that SAR11 could degrade dissolved organic
346 matter derived from oceanic phytoplankton. For example, the SAR11 genome
347 reportedly contains a gene for the degradation of phytoplankton-derived
348 dimethylsulfoniopropionate (Howard et al. 2006). Moreover, Nelson and Carlson (2012)
349 used stable isotope probing method to report that some SAR11 subclades utilized
350 organic substrates derived from *Synechococcus* in the open ocean. It suggested that
351 SAR11 lineage were actively involved in the degradation of organic matter derived
352 from phytoplankton in the South Pacific Ocean.
353 The cells detected by Alf968 probe accounted for 16% ± 10% of
354 DAPI-stained cells in the epipelagic layer, indicating that *Alphaproteobacteria*, except
355 for the SAR11 clade also contribute significantly to the bacterial standing stock. In
356 addition, alphaproteobacterial abundance was significantly correlated with salinity and

dissolved oxygen concentration, whereas environmental parameters barely affected SAR11 abundance (Table 3). These data suggest that environmental factors determining the distribution patterns of *Alphaproteobacteria* and SAR11 clade, differed. *Alphaproteobacteria* includes numerous lineages with functional characteristics distinct from SAR11, including *Roseobacter* and SAR116 clades, which are known as metabolic generalists with versatile mechanisms for energy acquisition from organic substrates (Newton et al. 2010; Oh et al. 2010). Thus, these functional differences may also affect distinct distribution patterns among alphaproteobacterial phylotypes in the Central South Pacific Ocean.

Some gammaproteobacterial lineages such as *Vibrio* and *Alteromonas*, are well known as copiotrophs, which can proliferate opportunistically in response to a supply of organic substrates from phytoplankton blooms (Riemann et al. 2000; Pinhassi et al. 2004; Tada et al. 2011; Teeling et al. 2012). However, *Gammaproteobacteria* includes some oligotrophic lineages such as the OM60/NOR5 clade, which represents aerobic anoxygenic photoheterotrophs (Yan et al. 2009) and cannot grow in nutrient-rich conditions (Cho and Giovannoni, 2004; Cho et al. 2007). In this study, the gammaproteobacterial abundance was negatively correlated with Chl *a* concentration and primary productivity (Tables 3, 4, and Supplementary Table 1), suggesting that the dominant gammaproteobacterial population in the southern part of South Pacific Ocean might be the oligotrophic lineages. In addition, our statistical analyses indicated that the dissolved oxygen concentration would be one of the primary factors affecting the gammaproteobacterial distribution (Tables 3 and 4). In previous report, the growth of

379 oligotrophic gammaproteobacterial lineages such as OM60/NOR5 strains was
380 stimulated by oxygen availability (Spring and Riedel, 2013). These data suggested that
381 dissolved oxygen concentration could be one of the primary factors determining the
382 gammaproteobacterial distribution in the South Pacific Ocean.
383 As for the latitudinal distribution of *Gammaproteobacteria*, their proportion
384 to the total bacteria and abundance drastically increased at Stations 8 and 9 (Fig. 3D,
385 Supplementary Figure 1). The results of hydrographic features such as salinity and
386 dissolved oxygen concentration (Fig. 2) indicated that the water mass belonging to
387 Stations 8 and 9 (low salinity and high dissolved oxygen concentration) differed from
388 those at other stations. Around this region, there is the eastward flow of the Eastern
389 Australian Current from the coasts of Western Australia and New Zealand into the
390 South Pacific Ocean (Godfrey et al. 1980; Oke et al. 2000; Tilburg et al. 2001). These
391 data suggest that the increase in *Gammaproteobacteria* may be explained by an
392 influence of the current system in this area. In addition, the western area of Station 8
393 was relatively productive based on weekly composite estimates of net primary
394 production (Supplementary Figure 2), and that might affect the abundance of
395 *Gammaproteobacteria*.
396 SAR86 is one of the ubiquitous clades of *Gammaproteobacteria* (Mary et al.
397 2006; Malmstrom et al. 2007), especially in the stratified euphotic layer (Morris et al.,
398 2005; Treusch et al. 2009). The present study showed that the percentage of SAR86
399 relatively increased in the surface layers of Stations 8 and 9 where relatively high
400 dissolved oxygen concentration and lower salinity and water temperature were observed

401 (Fig. 2). A previous metagenomic study showed that hydrographic features such as
402 water temperature would be the important factor determining the distribution of SAR86
403 subgroups (Dupont et al. 2012). In this study, however, their abundance increased with
404 dissolved oxygen concentration, and decreased with depth, salinity, and NH_4
405 concentration (Table 3), suggesting that the dissolved oxygen concentration, salinity,
406 and nutrient concentration could affect the SAR86 distribution in the South Pacific
407 Ocean. In addition, our multiple regression analysis showed that environmental factors
408 accounted for 38% of the variation in SAR86 distribution (Table 4), indicating that
409 external factors might also influence the spatial variability of SAR86.
410 Abundance of *Bacteroidetes* was positively correlated with water
411 temperature and negatively correlated with depth, suggesting that temperature gradient
412 with depth should be the critical factor determining the distribution pattern of
413 *Bacteroidetes* in the Pacific Ocean. Some previous studies revealed that *Bacteroidetes*
414 were more abundant in the surface ocean and their abundance decreased with depth
415 (Schattenhofer et al. 2009; Gómez-Pereira et al. 2010). In addition, *Bacteroidetes*
416 abundance significantly decreased with salinity in our survey area (Tables 3 and 4). In
417 fact, the proportion and abundance of *Bacteroidetes* decreased from 100–200 m depths
418 in the central part of the South Pacific Ocean (Stations 3 and 4), where there was a high
419 salinity water body (Fig. 2A, B). A previous study in the Mediterranean Sea showed the
420 contribution of *Bacteroidetes* lineage to the total community decreased with increasing
421 salinity (Díez-Vives et al. 2014). These data suggested that the physical parameter such
422 as the water temperature and salinity would be important factors determining the

423 distribution pattern of the *Bacteroidetes* in the South Pacific.

424 In the Atlantic Ocean, the contribution of *Bacteroidetes* to total prokaryotic
425 population increased in the Northern Atlantic Drift where a phytoplankton bloom
426 occurred (Schattenhofer et al. 2009). *Bacteroidetes* is known to be strongly associated
427 with natural or artificial phytoplankton blooms in coastal waters (West et al. 2008; Tada
428 et al. 2011; 2012). In our survey area, the *Bacteroidetes* abundance drastically increased
429 in the nutrient-rich equatorial upwelling region (Table 2 and Supplementary Figure 1).
430 However, our results showed that *Bacteroidetes* abundance was neither associated with
431 Chl *a* concentration nor primary productivity (Tables 3, 4, and Supplementary Table 1).
432 In fact, their relative abundance accounted for 5–10% of total cells even though in the
433 oligotrophic gyre under nutrient-limiting conditions (Fig. 3F). Several genome analyses
434 of marine *Bacteroidetes* lineages showed that they might possess the dual energy
435 acquisition strategies for living in both nutrient rich and poor environments (Bauer et al.
436 2006; González et al. 2008; González et al. 2011; Fernández-Gómez et al. 2013). They
437 can attach to the particles or phytoplankton cells to utilize the polymeric substrates
438 under the nutrient-rich condition (Bauer et al. 2006). In contrast, in the nutrient poor
439 water, they would obtain the energy from light using the proteorhodopsin gene, which
440 produce ATP by the light-driven proton pump (González et al. 2008; 2011). Therefore,
441 *Bacteroidetes* in the southern part of the South Pacific Ocean might be the distinct
442 physiological state, which optimized to nutrient-limiting conditions.

443

444 **4.2. Distribution of archaeal lineages**

445 This study revealed that the distribution of marine *Crenarchaeota* varied with latitude,
446 and this phylotype was the most abundant at 200 m depth at Station 1 (Fig. 4A). The
447 results obtained are consistent with previous studies (Karner et al. 2001; Teira et al.
448 2004; Herndl et al. 2005; Kirchman et al. 2007; Schattenhofer et al. 2009). It should be
449 noted that the probe GI-554 detects numerous chemoautotrophic lineages that can fix
450 CO_2 using ammonia as the electron donor and energy source (Herndl et al. 2005;
451 Francis et al. 2005), and thus could thrive in nutrient-rich layers (Könnecke et al. 2005;
452 Varela et al. 2008). However, our correlation analysis did not show a positive
453 relationship between crenarchaeotal abundance and the concentrations of NH_4 or NO_2
454 (Tables 2 and 3). In contrast, their abundance significantly increased with Chl *a*
455 concentration (Table 3). Previous isotopic studies showed that marine *Crenarchaeota*
456 possesses not only chemoautotrophic features, but heterotrophic as well (Teira et al.
457 2006b; Varela et al. 2008). In addition, the peaks in crenarchaeotal abundance and Chl *a*
458 concentration were detected in the surface layer of the Gulf of California (Beman et al.
459 2008). These data suggests that *Crenarchaeota* could be actively involved in organic
460 matter degradation around the euphotic zone in the Central South Pacific Ocean.
461 *Euryarchaeota* was relatively abundant within 100 m depth at Station 1,
462 where Chl. *a* concentration and primary productivity were relatively high (Fig. 4B). In
463 addition, the rank correlation and multiple regression analyses showed that the Chl. *a*
464 concentration could positively affected the euryarchaeotal abundance (Tables 3 and 4).
465 Our result is in good agreement with previous results obtained from the Mediterranean
466 Sea and arctic environments (Galand et al. 2008; Galand et al. 2010). In addition, recent

study has revealed that the marine *Euryarchaeota* associated with particulate organic matter or phytoplankton cells (Orsi et al. 2015). These data suggested that there could be a strong ecological linkage between *Euryarchaeota* and phytoplankton, and marine *Euryarchaeota* could be involved in the degradation of organic matter derived from phytoplankton in the equatorial region in the South Pacific Ocean.

4.3. Contribution of environmental factors to phylotype distribution

The results of multiple regression analysis revealed that the interpretability with environmental factors for prokaryotic distribution patterns differed among distinct phylotypes (Table 4). Some previous studies about global distribution patterns of prokaryotic phylotypes showed that the relative abundances of specific phylotypes varied with different gradients of environmental factors in the ocean (Wietz et al., 2010; Lefort and Gasol, 2013). These data suggested that the hydrographical gradients differently affect the phylotype-specific distribution patterns.

In addition, our study showed that the environmental factors analyzed explained 38% to 61% of the phylotype distribution, but large proportion of variance (39% to 62%) remained to be inexplicable. One plausible reason for this result is the lack of information of dissolved and particulate organic matter concentrations, which should be important factors controlling the heterotrophic bacterial production and standing stock in the Pacific Ocean (Yokokawa et al., 2013; Hasumi and Nagata, 2014). Therefore, the input of these organic matter data to the statistical analyses could effectively explain the phylotype distribution patterns by environmental factors.

5. Conclusions

The results from CARD-FISH analysis in this study revealed the basin-scale distribution of five bacterial and two archaeal phylotypes in the epipelagic layer of the Central South Pacific Ocean. We found that the latitudinal and depth distribution patterns of each phylotype differed in our survey area. Furthermore, Spearman's rank correlation and multiple regression analyses showed that the abundance of specific phylotypes was significantly correlated with several environmental factors. The SAR11 affiliated with *Alphaproteobacteria* was the dominant phylotype, and their abundance increased with Chl *a* concentration, indicating an ecological linkage between SAR11 and phytoplankton assemblages in the study area. We also found that all bacterial phylotypes, excluding *Gammaproteobacteria* but including SAR86, was more abundant in the equatorial region than in all other studied area, presumably due to the equatorial upwelling system. In contrast, *Gammaproteobacteria* and *Bacteroidetes* increased in the southern part in the Southern Pacific Ocean. *Gammaproteobacteria* and *Bacteroidetes* abundance significantly increased with dissolved oxygen concentration and water temperature, respectively. *Crenarchaeota* and *Euryarchaeota* were more abundant in the equatorial region, while they showed distinct vertical distribution patterns. In particular, *Euryarchaeota* abundance significantly decreased with depth, and increased with Chl. *a* concentration. These data suggest that hydrographic properties can principally determine the distribution of bacterial and archaeal phylotypes in the Central South Pacific Ocean.

Acknowledgments

We thank the captain and crew of the R/V *Hakuho-maru* for their support towards collecting samples for this study during cruise KH-13-7. This study was financially supported by Research Fellowships for Young Scientists (No. 13J04633 and No. 26740001) to Y. T. and Grants-in-Aid (No. 24121004) to K. S. from the Japan Society for the Promotion of Science.

References

Akaike H (1974) A new look at the statistical model identification. IEEE Trans Automat Contr 19(6):716-723

Amann R, Fuchs BM (2008) Single-cell identification in microbial communities by improved fluorescence in situ hybridization techniques. Nat Rev Microbiol 6(5):339-348

Amann RI, Binder BJ, Olson RJ, Chisholm SW, Devereux R, Stahl DA (1990) Combination of 16S rRNA-targeted oligonucleotide probes with flow cytometry for analyzing mixed microbial populations. Appl Environ Microbiol 56(6):1919-1925

Bauer M, Kube M, Teeling H, Richter M, Lombardot T, Allers E, Würdemann CA, Quast C, Kuhl H, Knaust F, Woebken D, Bischof K, Mussmann M, Choudhuri JV, Meyer F, Reinhardt R, Amann RI, Glöckner FO (2006) Whole genome analysis of the marine *Bacteroidetes* '*Gramella forsetii*' reveals adaptations to degradation of polymeric organic matter. Environ Microbiol 8(12):2201-2213

532 Beman JM, Popp BN, Francis CA (2008) Molecular and biogeochemical evidence for ammonia
533 oxidation by marine *Crenarchaeota* in the Gulf of California. ISME J 2(4):429-441
534 Campbell BJ, Waidner LA, Cottrell MT, Kirchman DL (2008) Abundant proteorhodopsin
535 genes in the North Atlantic Ocean. Environ Microbiol 10(1):99-109
536 Cho JC, Giovannoni SJ (2004) Cultivation and growth characteristics of a diverse group of
537 oligotrophic marine Gammaproteobacteria. Appl Environ Microbiol 70(1): 432-440
538 Cho JC, Stapels MD, Morris RM, Vergin KL, Schwalbach MS, Givan SA, Barofsky DF,
539 Giovannoni SJ (2007) Polyphyletic photosynthetic reaction centre genes in
540 oligotrophic marine Gammaproteobacteria. Environ Microbiol 9(6):1456-1463
541 del Giorgio PA, Gasol JM (2008) Physiological structure and single-cell activity in marine
542 Bacterioplankton. In: Kirchman DL (ed) Microbial Ecology of the Oceans, 2nd
543 Edition. John Wiley & Sons, Inc., Hoboken, New Jersey, pp. 243-298
544 Díez-Vives C, Gasol JM, Acinas SG (2014) Spatial and temporal variability among marine
545 Bacteroidetes populations in the NW Mediterranean Sea. Syst Appl Microbiol
546 37(1):68-78
547 Dupont CL, Rusch DB, Yooseph S, Lombardo MJ, Richter RA, Valas R, Novotny M,
548 Yee-Greenbaum J, Selengut JD, Haft DH Halpern AL, Lasken RS, Nealson K,
549 Friedman R, Venter JC (2012) Genomic insights to SAR86, an abundant and
550 uncultivated marine bacterial lineage. ISME J 6(6):1186-1199
551 Eiler A, Hayakawa DH, Church MJ, Karl DM, Rappé MS (2009) Dynamics of the SAR11
552 bacterioplankton lineage in relation to environmental conditions in the oligotrophic
553 North Pacific subtropical gyre. Environ Microbiol 11(9):2291-2300

554 Eilers H, Pernthaler J, Glöckner FO, Amann R (2000) Culturability and In situ abundance of
555 pelagic bacteria from the North Sea. Appl Environ Microbiol 66(7):3044-3051
556 Fazi S, Amalfitano S, Piccini C, Zoppini A, Puddu A, Pernthaler J (2008) Colonization of
557 overlaying water by bacteria from dry river sediments. Environ Microbiol
558 10(10):2760-2772
559 Fernández-Gómez B, Richter M, Schüler M, Pinhassi J, Acinas SG, González JM, Pedrós-Alió
560 C (2013) Ecology of marine Bacteroidetes: a comparative genomics approach.
561 ISME J 7(5):1026-1037
562 Francis CA, Roberts KJ, Beman JM, Santoro AE, Oakley BB (2005) Ubiquity and diversity of
563 ammonia-oxidizing archaea in water columns and sediments of the ocean. Proc Natl
564 Acad Sci USA 102(41):14683-14688
565 Galand PE, Gutiérrez-Provecho C, Massana R, Gasol JM, Casamayor EO (2010) Inter-annual
566 recurrence of archaeal assemblages in the coastal NW Mediterranean Sea (Blanes
567 Bay Microbial Observatory) Limnol Oceanogr 55(5):2117-2125
568 Galand PE, Lovejoy C, Pouliot J, Vincent WF (2008) Heterogeneous archaeal communities in
569 the particle-rich environment of an arctic shelf ecosystem. J Mar Syst
570 74(3):774-782.
571 Godfrey JS, Cresswell GR, Golding TJ, Pearce AF, Boyd R (1980) The separation of the East
572 Australian current. J Phys Oceanogr 10:430-440
573 Gómez-Consarnau L, González JM, Coll-Lladó M, Gourdon P, Pascher T, Neutze R,
574 Pedrós-Alió C, Pinhassi J (2007) Light stimulates growth of
575 proteorhodopsin-containing marine *Flavobacteria*. Nature 445(7124):210-213

576 Gómez-Pereira PR, Fuchs BM, Alonso C, Oliver MJ, van Beusekom JE, Amann R (2010)
577 Distinct flavobacterial communities in contrasting water masses of the North
578 Atlantic Ocean. ISME J 4(4):472-487
579 González JM, Fernández-Gómez B, Fernàndez-Guerra A, Gómez-Consarnau L, Sánchez O,
580 Coll-Lladó M, del Campo J, Escudero L, Rodríguez-Martínez R, Alonso-Sáez L,
581 Latasa M, Paulsen I, Nedashkovskaya O, Lekunberri I, Pinhassi J, Pedrós-Alió C
582 (2008) Genome analysis of the proteorhodopsin-containing marine bacterium
583 *Polaribacter* sp. MED152 (*Flavobacteria*). Proc Natl Acad Sci USA
584 105(25):8724-8729
585 González JM, Pinhassi J, Fernández-Gómez B, Coll-Lladó M, González-Velázquez M, Puigbò
586 P, Jaenicke S, Gómez-Consarnau L, Fernàndez-Guerra A, Goesmann A,
587 Pedrós-Alió C (2011) Genomics of the proteorhodopsin-containing marine
588 flavobacterium Dokdonia sp. strain MED134. Appl Environ Microbiol
589 77(24):8676-8686
590 Grossart HP, Levold F, Allgaier M, Simon M, Brinkhoff T (2005) Marine diatom species
591 harbour distinct bacterial communities. Environ Microbiol 7(6):860-873
592 Hama T, Miyazaki T, Ogawa Y, Iwakuma T, Takahashi M, Otsuki A, Ichimura S (1983)
593 Measurement of photosynthetic production of a marine phytoplankton population
594 using a stable 13C isotope. Marine Biology 73(1):31-36
595 Hasumi T, Nagata T (2014) Modeling the global cycle of marine dissolved organic matter and
596 its influence on marine productivity. Ecol Model 288(24):9-24

597 Herndl GJ, Reinthaler T, Teira E, van Aken H, Veth C, Pernthaler A, Pernthaler J (2005)
598 Contribution of Archaea to total prokaryotic production in the deep Atlantic Ocean.
599 Appl Environ Microbiol 71(5):2303-2309
600 Howard EC, Henriksen JR, Buchan A, Reisch CR, Bürgmann H, Welsh R, Ye W, González JM,
601 Mace K, Joye SB, Kiene RP, Whitman WB, Moran MA (2006) Bacterial taxa that
602 limit sulfur flux from the ocean. Science 314(5799):649-652
603 Iverson V, Morris RM, Frazar CD, Berthiaume CT, Morales RL, Armbrust EV (2012)
604 Untangling genomes from metagenomes: revealing an uncultured class of marine
605 *Euryarchaeota*. Science 335(6068):587-590
606 Karner MB, DeLong EF, Karl DM (2001) Archaeal dominance in the mesopelagic zone of the
607 Pacific Ocean. Nature 409(6819):507-510
608 Kirchman DL, Elifantz H, Dittel AI, Malmstrom RR, Cottrell MT (2007) Standing stocks and
609 activity of Archaea and Bacteria in the Western Arctic Ocean. Limnol Oceanogr
610 52(2):495-507
611 Könneke M, Bernhard AE, José R, Walker CB, Waterbury JB, Stahl DA (2005) Isolation of an
612 autotrophic ammonia-oxidizing marine archaeon. Nature 437(7058):543-546
613 Lefort T, Gasol JM (2013) Global-scale distributions of marine surface bacterioplankton groups
614 along gradients of salinity, temperature, and chlorophyll: a meta-analysis of
615 fluorescence in situ hybridization studies. Aquat Microb Ecol 70:111-130
616 Longhurst AR (2010) Ecological Geography of the Sea. 2nd Edition. Academic Press, USA, pp.
617 527

618 Malmstrom RR, Straza TRA, Cottrell MT, Kirchman DL (2007) Diversity, abundance, and
619 biomass production of bacterial groups in the Western Arctic Ocean. Aquat Microb
620 Ecol 47:45-55
621 Manz W, Amann R, Ludwig W, Vancanneyt M, Schleifer KH (1996) Application of a suite of
622 16S rRNA-specific oligonucleotide probes designed to investigate bacteria of the
623 phylum *Cytophaga-Flavobacter-Bacteroides* in the natural environment.
624 Microbiology 142(5):1097-1106
625 Manz W, Amann R, Ludwig W, Wagner M, Schleifer K-H (1992) Phylogenetic
626 oligodeoxynucleotide probes for the major subclasses of *Proteobacteria*: problems
627 and solutions. Syst Appl Microbiol 15(4):593-600
628 Mary I, Cummings D, Biegala I, Burkill P, Archer S, Zubkov M (2006) Seasonal dynamics of
629 bacterioplankton community structure at a coastal station in the Western English
630 Channel. Aquat Microb Ecol 42:119-126
631 Massana R, Murray AE, Preston CM, DeLong EF (1997) Vertical distribution and phylogenetic
632 characterization of marine planktonic *Archaea* in the Santa Barbara Channel. Appl
633 Environ Microbiol 63(1):50-56
634 Moore JK, Doney SC, Glover DM, Fung IY (2001) Iron cycling and nutrient-limitation patterns
635 in surface waters of the World Ocean. Deep Sea Res Part 2 Top Stud Oceanogr
636 49(2002):463-507
637 Morris RM, Frazar CD, Carlson CA (2012) Basin-scale patterns in the abundance of SAR11
638 subclades, marine *Actinobacteria* (OM1), members of the *Roseobacter* clade and
639 OCS116 in the South Atlantic. Environ Microbiol 14(5):1133-1144

640 Morris RM, Vergin KL, Cho J-C, Rappé MS, Carlson CA, Giovannoni SJ (2005) Temporal and
641 spatial response of bacterioplankton lineages to annual convective overturn at the
642 Bermuda Atlantic Time-series Study site. Limnol Oceanogr 50(5):1687-1696
643 Neef A (1997) Anwendung der in situ-Einzelzell-Identifizierung von Bakterien zur
644 Populationsanalyse in komplexen mikrobiellen Biozönosen. Dissertation,
645 Technische Universität München
646 Nelson CE, Carlson CA (2012) Tracking differential incorporation of dissolved organic carbon
647 types among diverse lineages of Sargasso Sea bacterioplankton. Environ Microbiol
648 14(6):1500-1516
649 Newton RJ, Griffin LE, Bowles KM, Meile C, Gifford S, Givens CE, Howard EC, King E,
650 Oakley CA, Reisch CR, Rinta-Kanto JM, Sharma S, Sun S, Varaljay V, Vila-Costa
651 M, Westrich JR, Moran MA (2010) Genome characteristics of a generalist marine
652 bacterial lineage. ISME J 4(6):784-798
653 Ogawa H, Fukuda R, Koike I (1999) Vertical distributions of dissolved organic carbon and
654 nitrogen in the Southern Ocean - a new high temperature combustion method and a
655 comparison with photo-oxidation. Deep Sea Res Part 1 Oceanogr Res Pap
656 46(10):1809-1826
657 Oh H-M, Kwon KK, Kang I, Kang SG, Lee JH, Kim SJ, Cho JC (2010) Complete genome
658 sequence of "*Candidatus Puniceispirillum marinum*" IMCC1322, a representative
659 of the SAR116 clade in the *Alphaproteobacteria*. J Bacteriol 192(12):3240-3241
660 Oke PR, Middleton JH (2000) Nutrient enrichment off Port Stephens: the role of the East
661 Australian Current. Cont Shelf Res 21(2001):587-606

662 Orsi WD, Smith JM, Wilcox HM, Swalwell JE, Carini P, Worden AZ, Santoro AE (2015)
663 Ecophysiology of uncultivated marine euryarchaea is linked to particulate organic
664 matter. ISME J 9(8):1747-1763
665 Pernthaler A, Preston CM, Pernthaler J, DeLong EF, Amann R (2002) Comparison of
666 fluorescently labeled oligonucleotide and polynucleotide probes for the detection of
667 pelagic marine *Bacteria* and *Archaea*. Appl Environ Microbiol 68(2):661-667
668 Pinhassi J, Sala MM, Havskum H, Peters F, Guadayol O, Malits A, Marrasé C (2004) Changes
669 in bacterioplankton composition under different phytoplankton regimens. Appl
670 Environ Microbiol 70(11):6753-6766
671 R Development Core Team (2011) R: A language and environment for statistical computing. R
672 Foundation for Statistical Computing, Vienna, Austria : the R Foundation for
673 Statistical Computing.
674 Rappé MS, Connon SA, Vergin KL, Giovannoni SJ (2002) Cultivation of the ubiquitous
675 SAR11 marine bacterioplankton clade. Nature 418(6898):630-633
676 Riemann L, Steward GF, Azam F (2000) Dynamics of bacterial community composition and
677 activity during a mesocosm diatom bloom. Appl Environ Microbiol 66(2):578-587
678 Schattenhofer M, Fuchs BM, Amann R, Zubkov MV, Tarran GA, Pernthaler J (2009)
679 Latitudinal distribution of prokaryotic picoplankton populations in the Atlantic
680 Ocean. Environ Microbiol 11(8):2078-2093
681 Shiozaki T, Furuya K, Kodama T, Takeda S (2009) Contribution of N2 fixation to new
682 production in the western North Pacific Ocean along 155°E. Mar Ecol Prog Ser
683 377:19-32

684 Spring S, Riedel T (2013) Mixotrophic growth of bacteriochlorophyll a-containing members of
685 the OM60/NOR5 clade of marine gammaproteobacteria is carbon-starvation
686 independent and correlates with the type of carbon source and oxygen availability.
687 BMC Microbiol 13(1):117
688 Suzuki R, Ishimaru T (1990) An improved method for the determination of phytoplankton
689 chlorophyll using N, N-dimethylformamide. J Oceanogr 46(4):190-194
690 Tada Y, Taniguchi A, Nagao I, Miki T, Uematsu M, Tsuda A, Hamasaki K (2011) Differing
691 growth responses of major phylogenetic groups of marine bacteria to natural
692 phytoplankton blooms in the western North Pacific Ocean. Appl Environ Microbiol
693 77(12):4055-4065
694 Tada Y, Taniguchi A, Sato-Takabe Y, Hamasaki K (2012) Growth and succession patterns of
695 major phylogenetic groups of marine bacteria during a mesocosm diatom bloom. J
696 Oceanogr 68:509-519
697 Teeling H, Fuchs BM, Becher D, Klockow C, Gardebrecht A, Bennke CM, Kassabgy M,
698 Huang S, Mann AJ, Waldmann J, Weber M, Klindworth A, Otto A, Lange J,
699 Bernhardt J, Reinsch C, Hecker M, Peplies J, Bockelmann FD, Callies U, Gerdts G,
700 Wichels A, Wiltshire KH, Glöckner FO, Schweder T, Amann R (2012)
701 Substrate-controlled succession of marine bacterioplankton populations induced by
702 a phytoplankton bloom. Science 336(6081):608-611
703 Teira E, Lebaron P, Van Aken H, Herndl GJ (2006a) Distribution and activity of *Bacteria* and
704 *Archaea* in the deep water masses of the North Atlantic. Limnol Oceanogr
705 51:2131-2144

706 Teira E, Reinthaler T, Pernthaler A, Pernthaler J, Herndl GJ (2004) Combining catalyzed
707 reporter deposition-fluorescence *in situ* hybridization and microautoradiography to
708 detect substrate utilization by bacteria and archaea in the deep ocean. Appl Environ
709 Microbiol 70(7):4411-4414
710 Teira E, Van Aken H, Veth C, Herndl GJ (2006b) Archaeal uptake of enantiomeric amino acids
711 in the meso‐and bathypelagic waters of the North Atlantic. Limnol Oceanogr
712 51:60-69
713 Tilburg CE, Hurlburt HE, O'Brien JJ, Shriver JF (2001) The dynamics of the East Australian
714 current system: the Tasman front, the East Auckland current, and the East Cape
715 current. J. Phys. Oceanogr 31:2917-2943
716 Treusch AH, Vergin KL, Finlay LA, Donatz MG, Burton RM, Carlson CA, Giovannoni SJ
717 (2009) Seasonality and vertical structure of microbial communities in an ocean gyre.
718 ISME J 3(10):1148-1163
719 Varela MM, Van Aken HM, Sintes E, Herndl GJ (2008) Latitudinal trends of Crenarchaeota
720 and Bacteria in the meso-and bathypelagic water masses of the Eastern North
721 Atlantic. Environ Microbiol 10(1):110-124
722 Venables WN, Ripley BD (2002). Modern Applied Statistics with S. 4th Edition.
723 Springer-Verlag, New York. pp. 495
724 Walker CB, de la Torre JR, Klotz MG, Urakawa H, Pinel N, Arp DJ, Brochier-Armanet C,
725 Chain PSG, Chan PP, Gollabgir A, Hemp J, Hügler M, Karr EA, Könneke M, Shin
726 M, Lawton TJ, Lowe T, Martens-Habbena W, Sayavedra-Soto LA, Lang D, Sievert
727 SM, Rosenzweig AC, Manning G, Stahl DA (2010) *Nitrosopumilus maritimus*

genome reveals unique mechanisms for nitrification and autotrophy in globally distributed marine *Crenarchaea*. Proc Natl Acad Sci USA 107(19):8818-8823

Wallner G, Amann R, Beisker W (1993) Optimizing fluorescent in situ hybridization with rRNA-targeted oligonucleotide probes for flow cytometric identification of microorganisms. Cytometry 14(2):136-143

Welschmeyer NA (1994) Fluorometric analysis of chlorophyll a in the presence of chlorophyll b and pheopigments. Limnol Oceanogr 39(8):1985-1992

West NJ, Obernosterer I, Zemb O, Lebaron P (2008) Major differences of bacterial diversity and activity inside and outside of a natural iron‐fertilized phytoplankton bloom in the Southern Ocean. Environ Microbiol 10(3):738-756

Wietz M, Gram L, Jørgensen B, Schramm A (2010) Latitudinal patterns in the abundance of major marine bacterioplankton groups. Aquat Microb Ecol 61:179-189

Yan S, Fuchs BM, Lenk S, Harder J, Wulf J, Jiao NZ, Amann R (2009) Biogeography and phylogeny of the NOR5/OM60 clade of Gammaproteobacteria. Syst Appl Microbiol 32(2):124-139

Yokokawa T, Yang Y, Motegi C, Nagata T (2013) Large-scale geographical variation in prokaryotic abundance and production in meso-and bathypelagic zones of the Central Pacific and Southern Ocean. Limnol Oceanogr 58(1):61-73

Yoshizawa S, Kawanabe A, Ito H, Kandori H, Kogure K (2012) Diversity and functional analysis of proteorhodopsin in marine *Flavobacteria*. Environ Microbiol 14(5):1240-1248

750 **Figure legends**

751 **Fig. 1** Stations 1 through 9 along cruise KH-13-7, charted by the R/V *Hakuho-maru*
752 between December 2013 and February 2014

753

754 **Fig. 2** Water temperature (A), salinity (B), dissolved oxygen (C), chlorophyll *a*
755 concentration (D), primary productivity (E), concentrations of NO_3 (F), NO_2 (G), NH_4
756 (H), PO_4 (I), and total prokaryotic abundance (J) at various depths (y-axis) along a
757 transect from north to south (x-axis). Dots indicate sampling points

758

759 **Fig. 3** Latitudinal and depth distribution of *Eubacteria* (A), *Alphaproteobacteria* (B),
760 SAR11 (C), *Gammaproteobacteria* (D), SAR86 (E), and *Bacteroidetes* (F), as % of
761 DAPI-stained cells. Dots indicate sampling points

762

763 **Fig. 4** Latitudinal and depth distribution of *Crenarchaeota* (A) and *Euryarchaeota* (B),
764 as % of DAPI-stained cells. Dots indicate sampling points

765

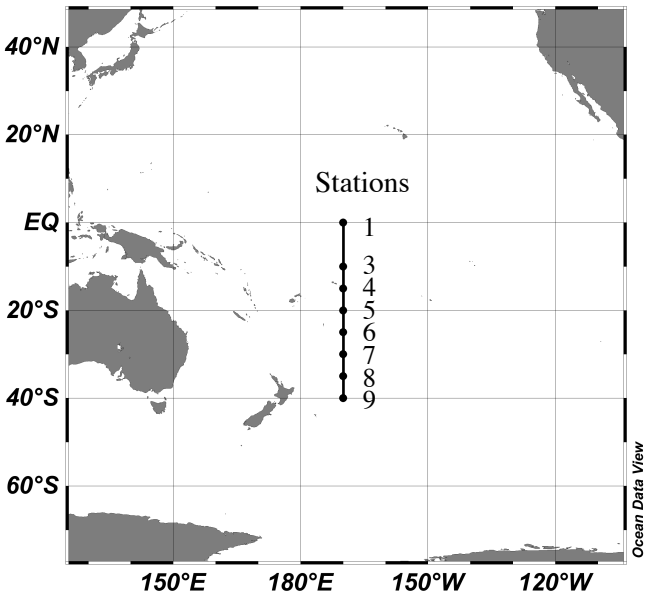

Fig. 1

Tada et al. (2016)

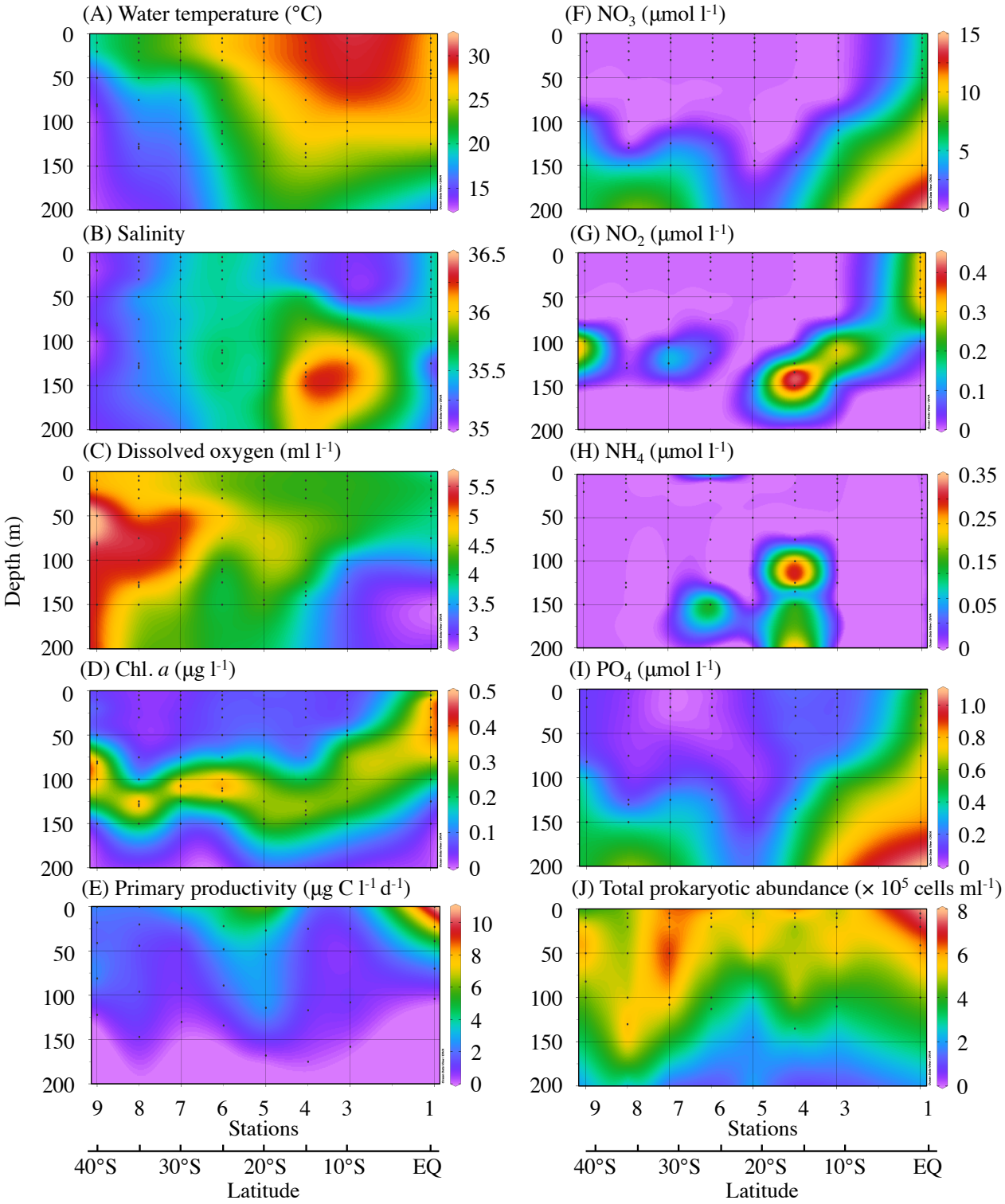

Fig. 2

Tada et al. (2016)

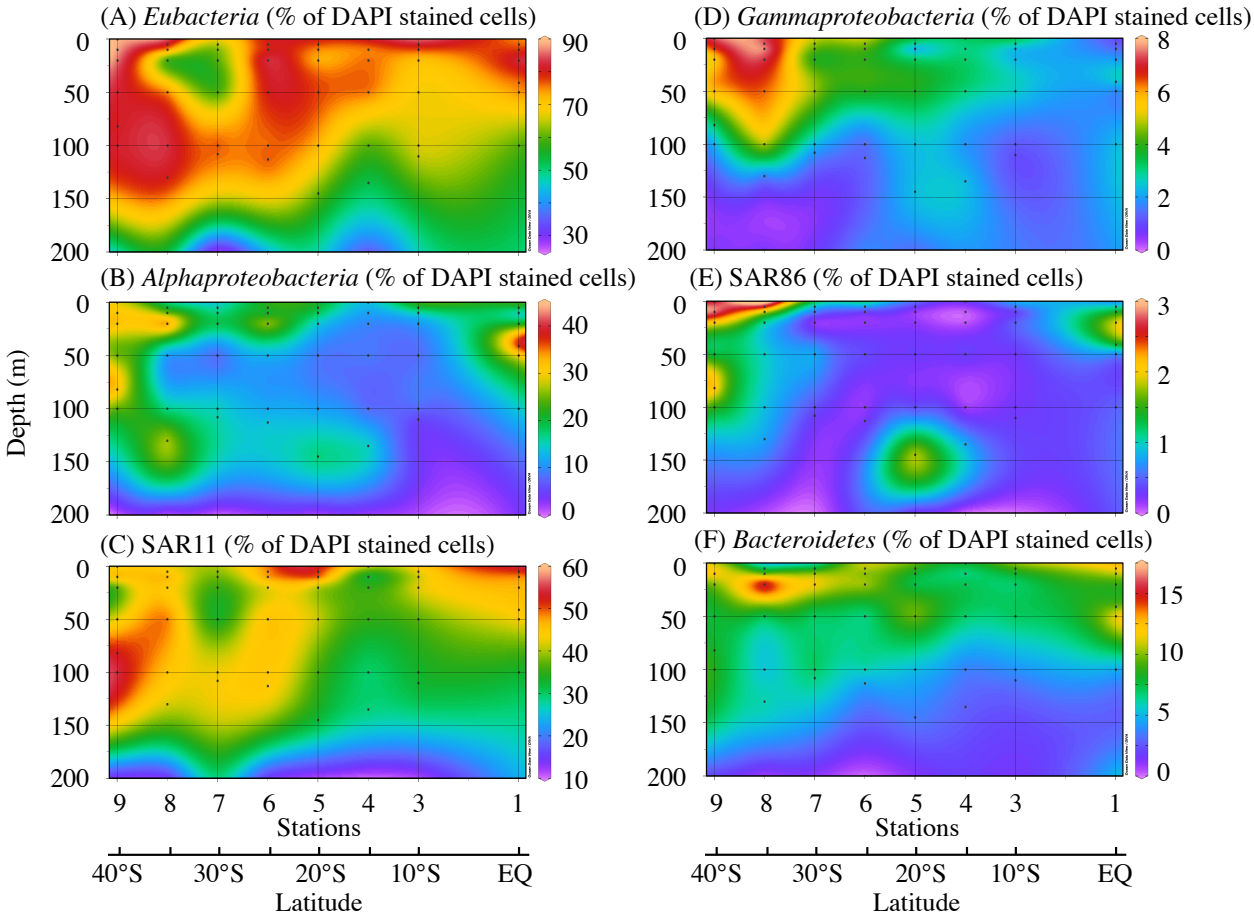

Fig. 3

Tada et al. (2016)

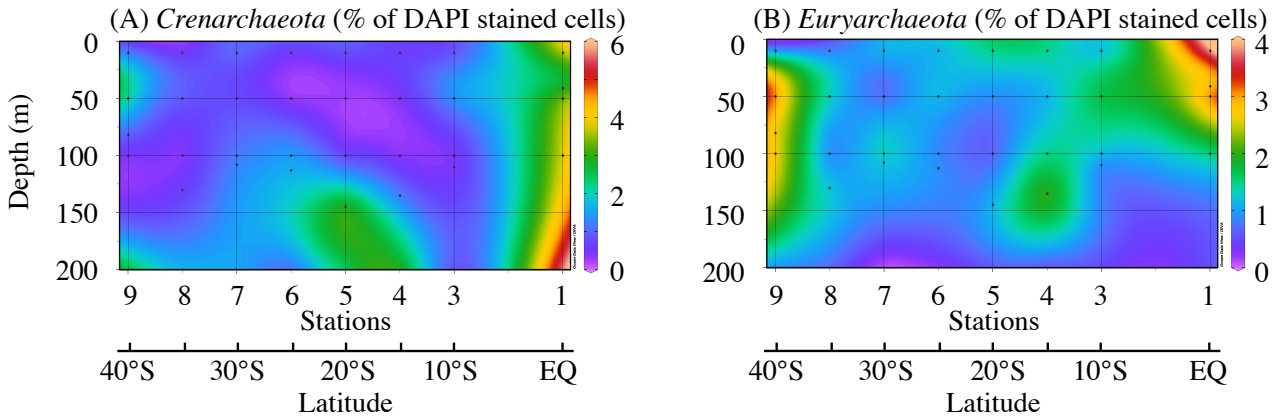

Fig. 4

Tada et al. (2016)

Supplementary materials

Supplementary Figure 1. Latitudinal and depth distribution of *Eubacteria* (A), *Alphaproteobacteria* (B), SAR11 (C), *Gammaproteobacteria* (D), SAR86 (E), *Bacteroidetes* (F), *Crenarchaeota* (G) and *Euryarchaeota* (H). Dots indicate sampling points

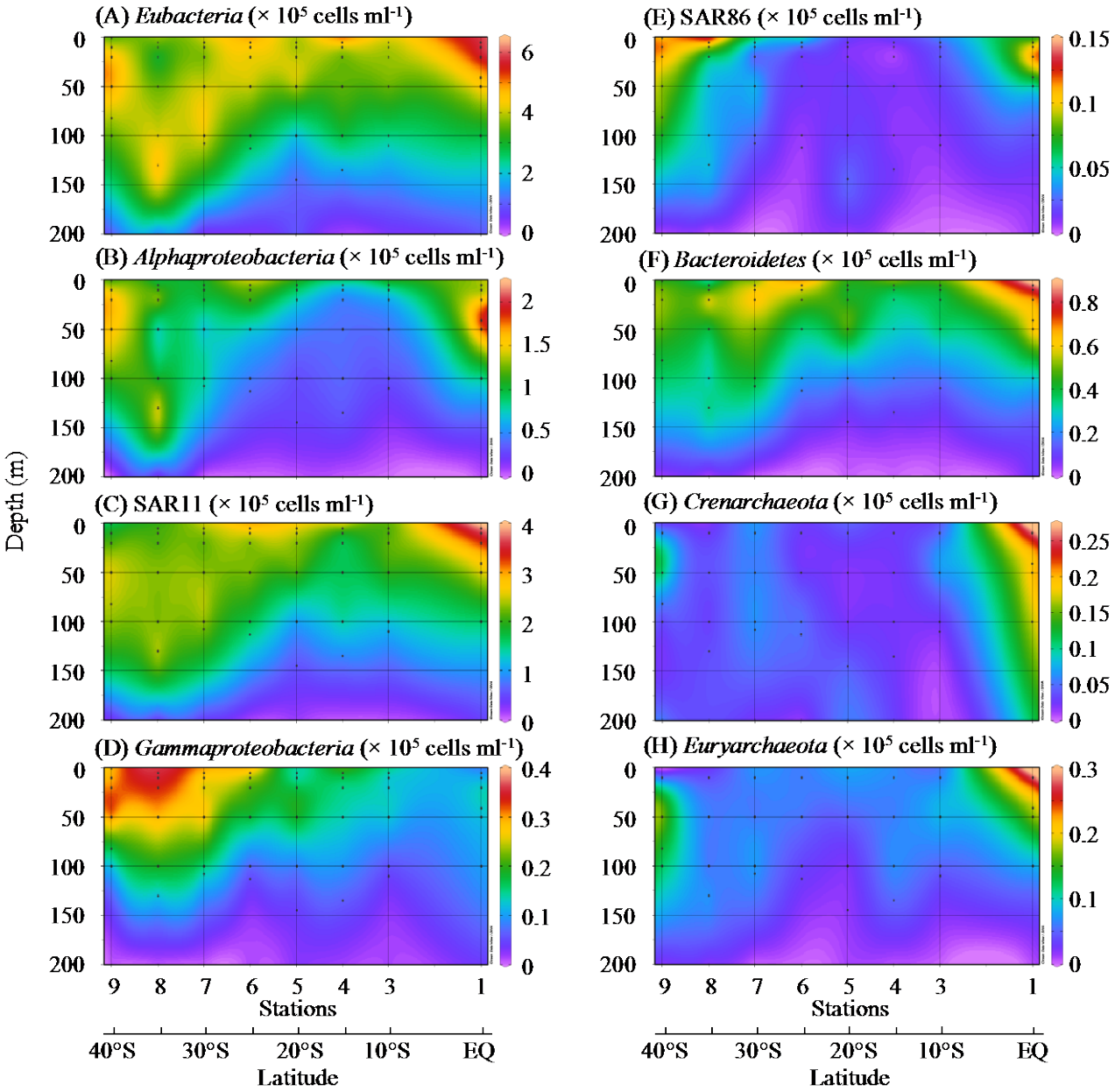

Supplementary Figure 2. Weekly composite estimates of net primary productivity (January 1–8, 2014), as derived from the Ocean Productivity database (http://www.science.oregonstate.edu/ocean.productivity/), along the transect from 175°E to 160°W at 35°S.

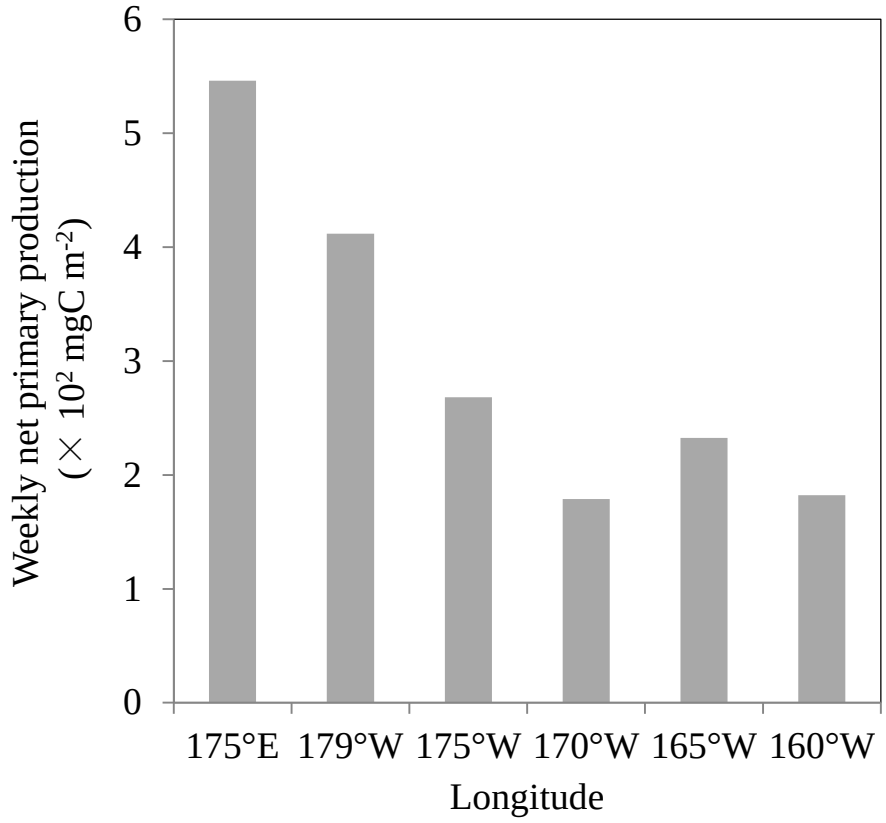

Supplementary Table 1. Spearman's rank correlation analysis of water-column integrated net primary productivity and abundance (depth-integrated values above 200 m) of total prokaryotes, *Bacteria*, and *Archaea* in the epipelagic zone of the central South Pacific.

	r value[b]								
Group and factor	Total prokaryotic abundance	*Eubacteria*	*Alphaproteobacteria*	SAR11	*Gammaproteobacteria*	SAR86	*Bacteroidetes*	*Crenarchaeota*	*Euryarchaeota*
Water-column integrated net primary production[a]	–0.21	0.17	0.31	0.24	0.12	0.19	0.38	–0.02	0.26

[a]Depth-integrated from 0.1% to 100% light intensity depths

Table 1. Station numbers, sampling dates, latitudes, longitudes, and environmental factors in surface waters at 5 m depth monitored during the KH-13-7 cruise aboard the R/V *Hakuho-maru*.

Station number	Sampling Date	Latitude (°S)	Longitude (°W)	Water temperature (°C)	Salinity	Dissolved oxygen concentration ($ml \cdot l^{-1}$)	Chl. *a* concentration ($\mu g \cdot l^{-1}$)	Water-column integrated net primary production[a] ($mg\ C \cdot m^{-2} \cdot d^{-1}$)	Depth of SCM layer (m)
St. 1	23-Dec-13	0	170	27.3	35.5	3.9	0.25	464	41
St. 3	26-Dec-13	10	170	30.3	35.1	4.2	0.06	147	110
St. 4[b]	2-Jan-14	15	170	29.0	35.2	4.3	0.07	186	135
St. 5	4-Jan-14	20	170	27.8	35.4	4.3	0.07	470	145
St. 6	7-Jan-14	25	170	26.3	35.5	4.4	0.07	339	113
St. 7	9-Jan-14	30	170	23.9	35.4	4.6	0.04	167	108
St. 8	12-Jan-14	35	170	22.0	35.2	4.8	0.03	216	130
St. 9[b]	13-Jan-14	40	170	19.8	35.1	4.9	0.06	227	82

[a]Depth-integrated from 0.1% to 100% light intensity depths

[b]Data of water temperature, salinity, and dissolved oxygen from 10 m depth, and that of Chl. *a* from 0 m depth

Chl *a*, chlorophyll *a*

SCM, subsurface chlorophyll maximum

Table 2. The water-column integrated cell number of each bacterial phylotype (depth-integrated values above 200 m) in the central South Pacific.

Station number	Water-column integrated cell numbers ($\times 10^{13}$ cells·m^{-2})							
	Bacteria (5–200 m)						Archaea (10–200 m)	
	Eubacteria	*Alphaproteobacteria*	SAR11	*Gammaproteobacteria*	SAR86	*Bacteroidetes*	*Crenarchaeota*	*Euryarchaeota*
St. 1	6.07	1.70	3.42	0.18	0.07	0.70	0.19	0.27
St. 3	4.58	0.56	2.39	0.14	0.02	0.38	0.09	0.04
St. 4*	4.70	0.68	2.25	0.18	0.02	0.36	0.10	0.04
St. 5	4.58	0.73	2.39	0.20	0.03	0.45	0.06	0.05
St. 6	5.28	1.00	2.95	0.19	0.02	0.44	0.07	0.05
St. 7	4.42	0.88	2.49	0.26	0.04	0.55	0.07	0.04
St. 8	6.96	1.93	3.90	0.36	0.08	0.64	0.10	0.05
St. 9*	6.50	1.90	3.59	0.31	0.12	0.65	0.19	0.08

* Used the cell number at 0 m depth instead at 5 m depth

Table 3. Spearman's rank correlation analysis of environmental factors and abundance of total prokaryotes, *Eubacteria* and Archaea in the epipelagic zone of the Central South Pacific Ocean.

Group and factor	Total prokaryotic abundance (n = 56)	*Rho* value[a] Bacteria (n = 56)						Archaea (n = 40)	
		Eubacteria	*Alphaproteobacteria*	SAR11	*Gammaproteobacteria*	SAR86	*Bacteroidetes*	*Crenarchaeota*	*Euryarchaeota*
Depth	–0.58**	–0.66**	–0.65**	–0.62**	–0.59**	–0.48**	–0.74**	–0.21	–0.64**
Water temperature	0.37**	0.32*	0.11	0.26	0.04	-0.1	0.30*	0.04	0.29
Salinity	–0.13	–0.23	–0.34*	–0.20	–0.40**	–0.39**	–0.28*	–0.34	–0.27
Dissolved oxygen conc.	0.16	0.23	0.29*	0.25	0.52**	0.37**	0.23	–0.02	0.24
Chl *a* conc.	0.21	0.23	0.22	0.27*	–0.47**	0.15	0.10	0.17	0.47**
NO_3	–0.38**	–0.41**	–0.29*	–0.33*	–0.74**	–0.18	–0.41**	0.13	–0.30
NO_2	–0.03	0.02	0.17	–0.34*	–0.37**	0.23	0.01	0.21	0.30
NH_4	–0.07	–0.19	–0.23	0.13	–0.18	–0.31*	–0.21	–0.14	–0.06
PO_4	–0.28*	–0.30*	–0.28*	–0.30*	–0.69**	–0.20	–0.37**	0.12	–0.13

[a]Level of significance: *, $P < 0.05$; **, $P < 0.01$

Chl *a*, chlorophyll *a*

11 Table 4. Multiple regression analysis of environmental factors and distribution of bacterial and archaeal phylotypes

Group and factor	Total prokaryotic abundance (n = 56)	Bacteria (n = 56)						Archaea (n = 40)	
		Eubacteria	*Alphaproteobacteria*	SAR11	*Gammaproteobacteria*	SAR86	*Bacteroidetes*	*Crenarchaeota*	*Euryarchaeota*
Multiple *R*-squared	0.57	0.63	0.48	0.61	0.59	0.38	0.51	0.49	0.57
F-statistic	13.5	21.8	9.4	19.8	18.6	10.5	13.3	6.6	9.1
P-value for model	< 0.001	< 0.001	< 0.001	< 0.001	< 0.001	< 0.001	< 0.001	< 0.001	< 0.001
Coefficient for each resource parameter[a]									
Water temperature	0.14***	0.13***	0.06***	0.12***	0.02***	NS	0.05***	0.02**	0.02***
Salinity	–0.04	–0.07***	–0.06**	–0.06**	NS	–0.01**	–0.03**	–0.01*	–0.01
Dissolved oxygen conc.	0.14**	0.10***	0.07***	0.09***	0.03***	0.01*	0.04***	0.01	0.03***
Chl *a* conc.	0.04*	0.07***	0.03	0.07***	–0.02**	NS	NS	0.01*	0.01**
NO_2	NS	NS	0.89	NS	0.19	0.17***	0.57**	NS	NS
NH_4	NS	NS	NS	NS	NS	NS	NS	NS	NS
PO_4	0.05	NS	NS	NS	NS	NS	NS	0.02**	0.02***

[a]Level of significance: *, $P < 0.05$; **, $P < 0.01$; ***, $P < 0.001$

Chl *a*, chlorophyll *a*

NS, not selected by Akaike information criteria

To meet assumptions of regression analysis, all parameters were log(x+1)-transformed.

12